RECOMMENDATION ITU-R S.1558

Methodologies for measuring epfd↓ caused by a non-geostationary-satellite orbit space station to verify compliance with operational epfd↓ limits

(Question ITU-R 236/4)

(2002)

The ITU Radiocommunication Assembly,

considering

a) that the World Radiocommunication Conference (Istanbul, 2000) (WRC-2000) adopted a combination of single-entry validation, single-entry operational and, for certain antenna sizes single-entry additional operational equivalent power-flux density↓ (epfd↓) limits, all of which are now contained in Article 22 of the Radio Regulations (RR), and also adopted the aggregate limits in Resolution 76 (WRC-2000), which apply to non-geostationary-satellite orbit fixed-satellite service (non-GSO FSS) systems to protect GSO networks in parts of the frequency range 10.7-30 GHz;

b) that the operational epfd↓ limits were adopted by WRC-2000 to protect operational GSO FSS networks from interference levels which may result in severe degradation in performance;

c) that operational epfd↓ limits were also adopted by WRC-2000 to protect operational GSO FSS networks employing adaptive coding from interference levels which may result in loss of capacity, which is considered a severe degradation;

d) that Resolution 137 (WRC-2000) invites the ITU-R to develop, with the aim of completion by 2003, measurement methods which may be used by administrations to verify compliance of an individual non-GSO FSS system with these operational limits;

e) that, as a consequence of those measurements, a non-GSO system causing interference may have to reduce its epfd↓ power levels towards the affected GSO earth station to meet the single-entry operational epfd↓ limits unless otherwise agreed by the concerned administrations;

f) that compliance of a non-GSO FSS system with the single-entry operational epfd↓ limits is not subject to verification by the ITU-R;

g) that the determination of whether a non-GSO FSS system is exceeding the operational epfd↓ limit into an operating GSO earth station would be made by individual administrations and their GSO network operators;

h) that the worst-case occurrences of events exceeding the operational limits are likely to be of short duration (from a fraction of a second to a few seconds) with a repeat period ranging from several days to weeks, depending on the orbital characteristics of the non-GSO system;

j) that the loss of synchronization or severe degradation may be used as a trigger for the application of a methodology for checking whether the operational limits are met;

k) that a reliable means of measuring the actual interference corresponding to the epfd↓ produced by a non-GSO FSS system into the operational GSO earth station experiencing interference would assist administrations and operators in determining whether a non-GSO system is exceeding the operational epfd↓ limit;

l) that measurement procedures have inherent accuracy and operational limitations which have to be taken into account during the measurement process,

noting

a) that regulatory procedures are being developed to enable the quick resolution of any proven instance of the operational epfd↓ limits being exceeded;

b) that Recommendation ITU-R S.1527 has been developed enabling the identification of satellites belonging to a particular non-GSO system;

c) that Recommendation ITU-R S.1554 has been developed in order to assess the overall accuracy of epfd↓ measurements,

recommends

1 that the methodologies described in Annex 1 be used by individual administrations and their GSO system operators to determine if non-GSO FSS interference exceeds the operational epfd↓ limits into an operating GSO earth station.

NOTE 1 – Other measurement methods may be identified. In due course it may be appropriate to add such methods to this Recommendation.

ANNEX 1

1 Introduction

This Annex provides methodologies to enable the measurement of the power flux-density (pfd) level emitted from a non-GSO space station incident at the antenna aperture of an operational GSO earth station receiver sharing the same frequency bands. This level can then be compared with operational epfd↓ limits provided in RR Article 22 to determine whether the non-GSO space station is exceeding these limits. These limits should be met in order to comply with RR No. 22.5I and also to protect GSO FSS links from suffering loss of synchronization or degraded performance[1] due to the passage of non-GSO satellites close to or within the main beam of the GSO earth station antenna.

Three methods have been identified, each having advantages and disadvantages. Details of each method are provided in Sections 2, 3 and 4.

One or more of these methods can be invoked if a loss of synchronization or degraded performance occurred at a GSO earth station at an unexpected time (i.e. not obviously caused by a high rain or scintillation fade, a sun outage event, a terrestrial interference source such as radar, or an event caused by equipment failure and/or associated switch-over). The GSO satellite operator would then

[1] This includes protection of GSO FSS systems employing adaptive coding from loss of capacity.

determine, via ephemeris data whether an in-line or near in-line event had occurred at the location of the site incurring the loss of synchronization and communicate the results of the measurement to the non-GSO operator concerned.

It is expected that the occurrence of in-line or near in-line events will be rare and it is essential that either the methods described in Sections 2, 3 and 4 are fully automated or that the time of a repeat occurrence can be accurately determined.

The method in Section 2 is a procedure for identifying that there may be a loss of synchronization or severe degradation problem and that the operational epfd↓ limits may be exceeded. If it is judged that the problem may be due to peak interference from a non-GSO system, Method 2 or 3 may be employed to measure the peak epfd↓ level. Method 1 requires a minimal use of staff and equipment resources.

More detailed methods are presented in Sections 3 and 4. These can either be used as standalone methods of determining the epfd↓ more accurately or as a follow-on procedure from the method in Section 2. None of these methods assume the presence of a dedicated non-GSO pilot signal.

In Section 3 the interference level is measured in frequency bands between adjacent carriers which have suffered loss of synchronization or degraded performance[1]. These methods assume that the interfering traffic carrier is sufficiently broadband to include both the affected carrier and the guardband between it and the adjacent carrier, and that the carrier sideband level is sufficiently attenuated to be able to measure the interference power level in the guardband. The method is also valid for the case where multiple carriers, of the non-GSO system in frequency division multiple access (FDMA), span both the affected carrier and the guardband. If the non-GSO carrier is sufficiently broadband or there are multiple non-GSO carriers in FDMA, the effects due to Doppler frequency shift on the non-GSO carrier are minimized. The preferred realization of this approach uses a reference earth station (e.g. a carrier system monitor (CSM) earth station). The key advantage of using the CSM earth station is that it avoids the need to know the gain of the affected earth station receive chain.

Section 4 contains some techniques which make use of auto- and cross-correlation techniques to derive the interference level from a measurement of the non-GSO carrier in the presence of the affected GSO carrier when the non-GSO carrier level is well below the GSO carrier level. The choice of which technique in Section 4 to use depends on the level of the *a priori* knowledge of the non-GSO satellite signal being separately available. These techniques are more complicated for the GSO operator to carry out because they are accomplished at the centre frequency of the GSO carrier.

Calibration is an important factor in assessing the overall accuracy of each of these techniques. Recommendation ITU-R S.1554 includes some information on this matter.

2 Method 1: A rapid technique based on loss of synchronization

The following method is a simplified procedure for identifying a possible exceedance of the operational epfd↓ limits. This technique is sufficient to show that the operational limits may have been exceeded in the case where a loss of synchronization in the operating GSO carrier has

---

[1] This includes protection of GSO FSS systems employing adaptive coding from loss of capacity.

occurred. More comprehensive measurement procedures may be required to accurately determine the epfd↓ levels generated by the non-GSO system into the operational GSO earth station antenna.

The following steps will lead to a determination of whether the operational limits have been exceeded by a non-GSO system.

Step 1: Record the date and coordinated universal time (UTC) of the loss of synchronization as accurately as possible, as well as the duration of the loss of synchronization under clear sky and nominal operating conditions (see Note 1) (no sun outage, no switch-over, equipment failure etc.).

Step 2: Correlate the time of the loss of synchronization with the presence of the non-GSO satellite close to or within the main beam of the GSO earth station antenna by using the ephemeris data (see Note 2) of the non-GSO and GSO satellite systems.

Step 3: Verify the C/N of the GSO carrier during clear sky conditions and verify the C/N threshold at which loss of synchronization of the demodulator (see Note 3) occurs to ensure that there are not any technical problems with the earth station.

Step 4: Compute the epfd↓ received at the antenna aperture during the synchronization loss in Step 1 using: the link budget of the GSO carrier, the C/N synchronization loss threshold of the receiving demodulator and the G/T of the earth station.

Step 5: Establish the times of subsequent non-GSO satellite passes and go back to Step 1 until the correlation between the event of non-GSO satellite pass close to or through the GSO earth station main beam and a loss of synchronization appears to be confirmed.

Step 6: If there is correlation between the event of a non-GSO satellite pass and a loss of synchronization, and the calculation of the epfd↓ made in Step 4 shows that the non-GSO system is probably exceeding the operational epfd↓ limits, the GSO operator may decide to use a more comprehensive method to determine the epfd↓ levels generated by the non-GSO system into its operational earth station more accurately. The GSO operator may also decide to advise the non-GSO system operator that his system is causing a degradation to the GSO earth station.

This method contains inherent uncertainties not present in the other methods, i.e. uncertainty in the $C/(N + I)$ at which a demodulator loses synchronization for a given bit rate, type of modulation and forward error correction (FEC), uncertainty in the C/N ratio during an in-line event, and variation in C/N threshold, at which loss of synchronization occurs, with the duration of interference peak.

However, when a loss of synchronization is recorded and correlated with ephemeris data, an in-line event can be assumed to have occurred.

NOTE 1 – It will be important to note the weather for the GSO earth station location.

NOTE 2 – It is assumed that the non-GSO ephemeris data is available.

NOTE 3 – This can be done by checking the E_b/N_0 readout of the demodulator.

3 Method 2: epfd↓ measurement technique using a calibrated reference earth station

3.1 Principle of the measurement procedure

The measurement of the epfd↓ at an earth station requires the calibration of the receive earth station receive chain to provide a conversion factor that enables the translation of power measurements taken at an RF or IF point in the receive chain into an epfd↓ value at the receive antenna aperture. The power level measurement is made either in absolute terms or relative to some known reference

level. The latter approach is used in the methods described in Section 3 through the cooperation of a well-calibrated reference earth station. This eliminates the need to know the precise antenna gain and receive chain gain for the earth station under test.

The standard approach for satellite system monitoring involves a power measurement using either a power meter, spectrum analyser or a digital signal processing (DSP) device. The measurements consist of four basic parts:

– gain calibration of the receive signal path;

– non-GSO interference plus noise measurement;

– noise power measurement to determine the earth station noise level;

– fade measurement using GSO beacon or telemetry channel.

Several of these measurements have to be done in rapid succession, before the environment changes. Section 3 describes a preferred realization of this methodology which makes use of a well-calibrated reference earth station.

This measurement procedure requires the cooperation of a well-calibrated GSO FSS earth station that, simultaneously with the affected GSO earth station, can accurately measure the equivalent isotropically radiated power (e.i.r.p.) of the GSO carrier and/or a GSO beacon signal. Most GSO FSS satellite operators have CSM earth stations that measure the e.i.r.p. of each operational carrier to ensure the satellite transponder is operating at its planned input and output back-off point. By accurately calibrating the peak e.i.r.p. of the wanted carrier at the satellite, the e.i.r.p. in the direction of the interfered with GSO earth station can be calculated. This procedure takes advantage of the accurate e.i.r.p. measurements of the CSM by calibrating the e.i.r.p. of the interfered with GSO FSS carrier or a GSO beacon. The GSO beacon could be either one generated on the satellite or an unmodulated carrier inserted between the two carriers by an uplink earth station. If a reference earth station is not available, the affected earth station may be able to incorporate equipment to accurately calibrate the gain of its receive signal path.

The following are the steps which could be undertaken in implementing this procedure:

Step 1: Firstly, the GSO carrier level or beacon signal is monitored and the carrier-to-noise (C_{GSO}/N) level is derived from a measurement of ($C_{GSO} + N$)/N using a suitable power measuring device (see equation (1)). This measurement can be carried out automatically and preferably shortly before and immediately following a measured burst of non-GSO interference. This level relates to the pfd incident on the antenna from the GSO satellite, which is easily calculated (see equation (2)).

The mathematical relationship between ($I + N$)/N ratio ($I_{non\text{-}GSO} + N$)/N (dB) and I/N ratio ($I_{non\text{-}GSO} + N$)/N (dB) is given in equation (1):

$$\frac{I_{non\text{-}GSO}}{N} = 10 \log \left(10^{0.1 \left(\frac{I_{non\text{-}GSO} + N}{N} \right)} - 1 \right) \quad \text{dB}$$

$$\frac{I_{non\text{-}GSO} + N}{N} = 10 \log \left(10^{0.1 \left(\frac{I_{non\text{-}GSO}}{N} \right)} + 1 \right) \quad \text{dB} \qquad (1)$$

$$pfd_{GSO} = E_s - (L_s + L_{abs}) \quad \text{dB(W/m}^2\text{)} \qquad (2)$$

where:

pfd_{GSO}: pfd of the received GSO signal at antenna aperture

E_s: GSO satellite e.i.r.p. in the direction of the receiving test antenna (dBW)

L_{abs}: gaseous atmospheric absorption (dB)

L_s: spreading loss, which is calculated using the equation:

$$L_s = 10 \log(4\pi d^2) \qquad \text{dB(m}^2\text{)}$$

where d is the distance from test antenna to GSO satellite (m).

Step 2: The second step is to measure the peak non-GSO interference noise level and then subtract the background GSO satellite noise and other noise contributions. The noise level due to the non-GSO interference can then be referenced to the measured level from the GSO satellite carrier or beacon and, as the gains and losses throughout the entire receive chain are the same for both measurements performed sufficiently close together in time and frequency, the non-GSO epfd↓ level can then be reliably calculated. The calculation of non-GSO epfd↓ from $(I_{non\text{-}GSO} + N)/N$ (dB) measurements is given in equation (3). The whole of this process can be automated – this is an essential requirement of such a method in an unmanned station or where multiple measurements have to be taken.

$$epfd_{non\text{-}GSO} = pfd_{GSO} + \left(\frac{I_{non\text{-}GSO}}{N} - \frac{C_{GSO}}{N} \right) \qquad \text{dB(W/(m}^2 \cdot \text{40 kHz))} \qquad (3)$$

A typical measurement configuration for this technique is shown in Fig. 1.

3.2 Noise + interference power measurement

As described above, if a reference (CSM) earth station is available this measurement procedure does not require the absolute measurement of the carrier power but only an accurate $(C + N)/N$ measurement.

This method assumes that the interference level is measured at frequency bands between adjacent GSO carriers which have suffered loss of synchronization. Since the GSO signal cannot be turned off, the bands between carriers provide the next best measurement opportunity after the option of measuring the affected carrier frequency. However, in some cases it may not be possible to measure between the carriers, and the next closest carriers should be used. In this case, inaccuracies due to frequency scaling should be taken into account.

With the approach described in Section 3, the level of epfd↓ which can be measured is limited because the interference is assumed to be wideband digital with uniform power spectral density (psd). The only way that the interference could be measured with improved margin above the noise floor and thus with improved accuracy would be for the non-GSO to provide a downlink beacon. This non-GSO beacon would have to be narrow-band and have high power spectral density and be related to the power in a carrier representing the 100% loading situation by some constant value. The trade-off between the gains in improved ease of measurement and accuracy, and the increased complexity in non-GSO satellite design, has not yet been studied. To enable this, the GSO community would have to vacate a 40 kHz (40 kHz is for the 10-11 GHz band and 40 kHz or 1 MHz are for the 20 GHz band) slot and the non-GSO operator would have to design its overall frequency plan to insert the beacon into each downlink beam on every satellite.

FIGURE 1

Typical measurement configuration

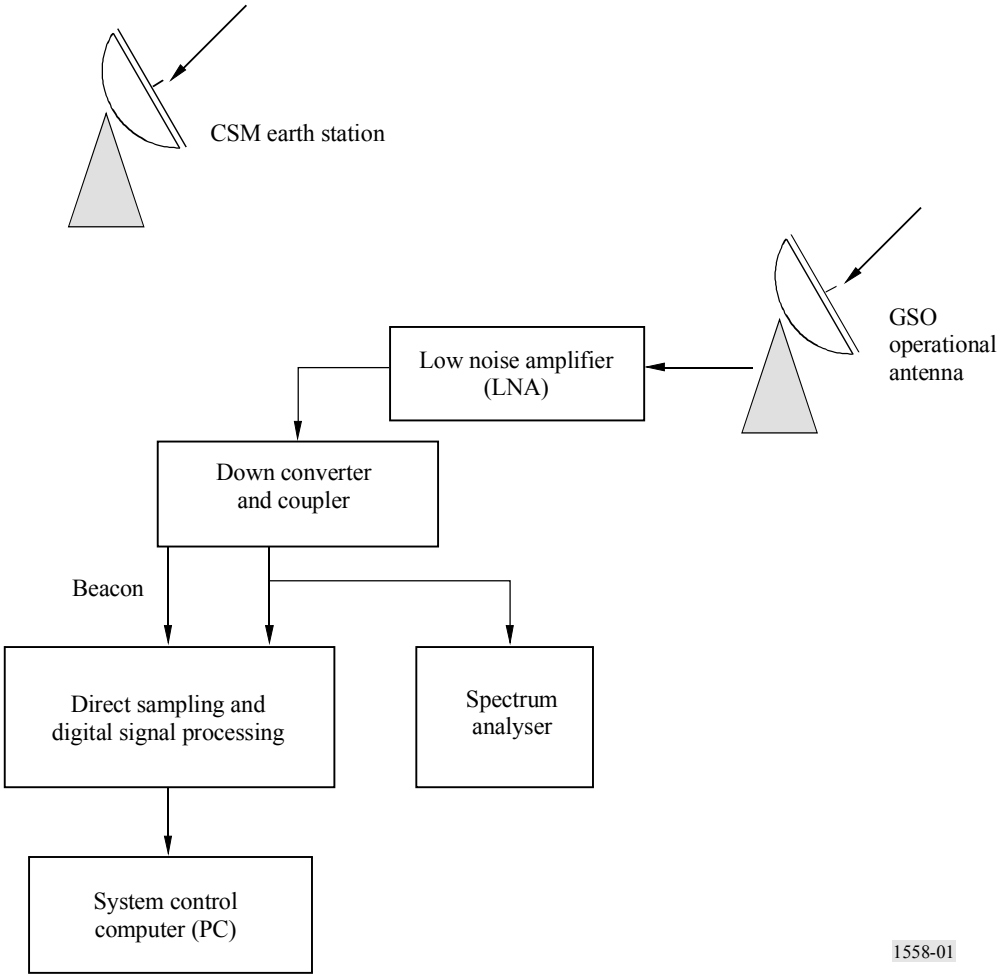

A typical measurement configuration is shown in Fig. 1. It is assumed that the interfering non-GSO signal is broadband and would cover more than one GSO FSS carrier, as shown in Fig. 2. The power measurements of the carrier plus noise ($C + N$), and noise levels would be taken in a 40 kHz bandwidth in the time period immediately before and after the interference event. These power measurements could be taken with a high quality analogue spectrum analyser or a sophisticated vector/spectrum analyser with a digital sampling system (DSS) as shown in Fig. 1.

FIGURE 2

Typical frequency plan for a 14/11 GHz band transponder loaded with GSO 2 Mbit/s carriers and interference from a broadband non-GSO code division multiple access (CDMA) signal

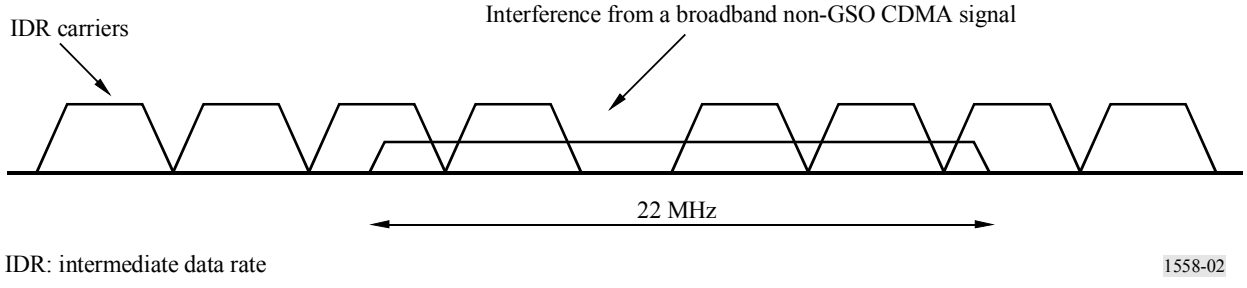

IDR: intermediate data rate

Figure 3 shows the power spectrum of two 2 Mbit/s digital carriers as measured by a DSS. The spectrum shown spans across a frequency range of 2 MHz and was taken in between two adjacent digital carriers of 2 MHz each. The guardband between the two carriers is now visible and this area represents the noise floor of the received signal. This Figure shows that a good estimate of the signal power and the noise floor in a 40 kHz bandwidth can be measured within as short a period as 64 ms, which would be required for a 10 m antenna with a beamwidth of a few tenths of a degree.

FIGURE 3

DSS measurements with external noise interference

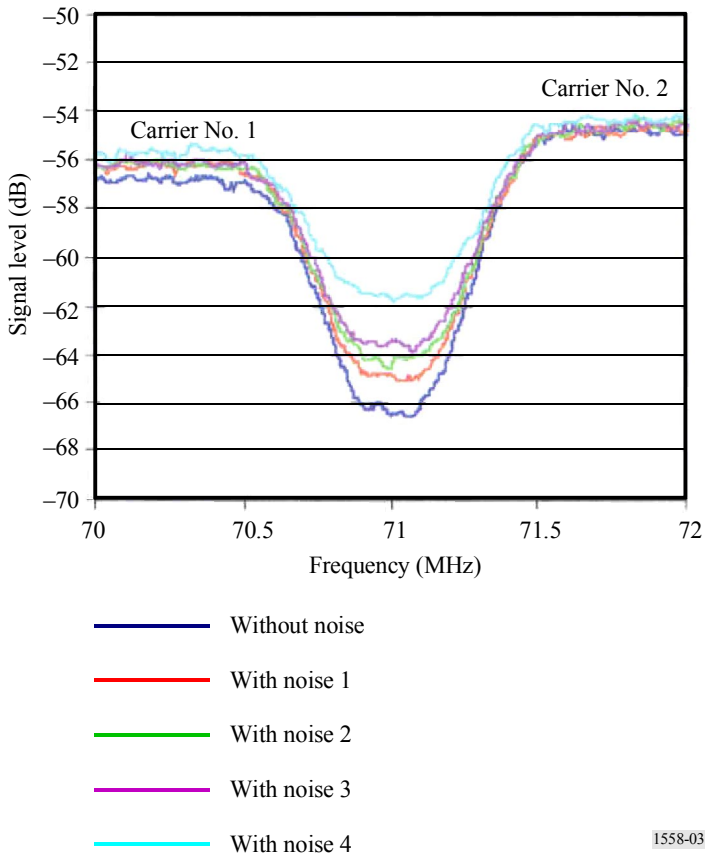

Figure 3 also shows the increase in the power density level between the carriers as the interference adds to the receiver noise. This measurement illustrates how the low level interference signals in an unoccupied area of a satellite transponder would be used to measure the interference. The I/N for the four cases are: –3.9, –1.6, 0.0 and 2.8 dB.

3.3 Non-GSO and GSO satellite ephemeris data

An important factor in this measurement procedure is the determination of the predicted non-GSO interference event. The determination of the interference event using the most up-to-date publicly available ephemeris data would be essential to allow accurate epfd↓ measurement of all expected peak levels since the noise and signal levels must be monitored immediately before and after the interference event. A calibration of the receive chain of the affected GSO earth station by the CSM earth station would need to be carried out near in time to the peak interference event. Since most test equipment has limited memory capabilities the measurement window is critical in ensuring the recording time of the measurements will cover the interference event.

Further information on the procedure to correlate the non-GSO in-line or near in-line event with the GSO main beam is given in Recommendation ITU-R S.1527.

3.4 GSO satellite beacon measurement

During the non-GSO epfd↓ measurements, fading or variations in the carrier and noise could occur. To ensure the epfd↓ measurements are carried out under clear-sky conditions, both the interfered with earth station and the CSM earth station would continuously monitor the GSO satellite beacon. If there are several beacons, the closest beacon to the interference frequency would be used. Variations in the level of the beacon could indicate rain or atmospheric affects, satellite or earth station tracking variations, etc. Depending on the cause of the variations and whether they would affect the interference measurement, the measurement may have to be repeated.

3.5 Effect of antenna size on the ability to perform measurements of operational epfd↓ levels

The smaller the GSO earth station antenna, the more difficult it will be to perform the measurement of the interference power relating to the epfd↓ incident on the antenna. This is because the levels of interference power density received from non-GSO FSS systems conforming to the operational limits in the Tables of RR Article 22 are likely to be below the thermal noise floor for the smaller antennas.

Table 1 shows the unwanted *I*/*N* ratios which correspond to the operational single entry epfd↓ limits in RR Article 22.

TABLE 1

Operational limits expressed as unwanted *I*/*N* which may be measured during an in-line event(1)

Frequency band (GHz)	epfd↓ level (not to be exceeded for 100% of the time)	GSO earth station antenna diameter (m) or antenna gain (dBi)	Unwanted interference power density/noise power density ratio(2) (*I*/*N*) (dB)
10.7-12.75	−163 dB(W/(m^2 · 40 kHz)	3 m	4.4
10.7-12.75	−166 dB(W/(m^2 · 40 kHz)	6 m	7.5
10.7-12.75	−167.5 dB(W/(m^2 · 40 kHz)	9 m	9.5
10.7-12.75	−169.5 dB(W/(m^2 · 40 kHz)	≥ 18 m	≥ 13.5
17.8-18.6	−150 dB(W/(m^2 · MHz)	≥ 49 dBi	≥ −3
19.7-20.2	−143 dB(W/(m^2 · MHz)	≥ 49 dBi	≥ 3.2
19.7-20.2	−143 dB(W/(m^2 · MHz)	43 dBi	−2.8

(1) The limits in Table 1 apply to GSO satellites having orbital inclinations of ≤2.5°.

(2) The actual *I*/*N* will be lower due to additional intra-system noise on both the downlink of the wanted GSO and interfering non-GSO satellites which will add to the thermal noise of the reference antenna and its receiver. Digital modulation and an occupied bandwidth at least equal to reference bandwidth on the non-GSO interference has been assumed in all cases. A receiving antenna efficiency of 65% and a receiving system noise temperature of 150 K for the 10.7-12.75 GHz frequency range and 250 K for the 17.8-20.2 GHz frequency range have been assumed in all cases.

3.6 Practical example of the measurement procedures described in Section 3

3.6.1 Description of measurement set-up and conduct of trials

In order to validate the method described in Section 3, a week-long exercise took place via a GSO satellite using typical GSO carriers and a wideband interfering signal whose amplitude and duration were controlled by a computer.

The experiment was carried out in the 14/11 GHz band via a GSO satellite at 342° E from Goonhilly earth station in the South-West of the United Kingdom. A CSM earth station at Fucino in Italy was also involved and this was located close to the centre of the beam.

Two standard INTELSAT IDR carriers (quadrature phase shift keying (QPSK) modulation with rate-3/4 FEC) were transmitted via a 19 m antenna, and received by a 5.5 m antenna. A signal having a power profile similar to the non-GSO interference during in-line passes was generated, using a PSK modulator whose output was routed to an uplinking 3.7 m antenna via a computer-controlled PIN diode attenuator. The shapes of the peaks thus generated were controlled by the computer to match the amplitude/time profile of the interference from a non-GSO satellite at 1 470 km altitude and 53° inclination during a pass through the beam centre of a 5.5 m earth station antenna located at Goonhilly and operating to a GSO satellite at 342° E. To demonstrate the feasibility of measurements in the case of the narrowest peaks, a few measurements were also carried out using an amplitude/time profile similar to that of non-GSO interference during a pass through the beam of a 19 m antenna on the Equator operating at 90° elevation angle. The interference signal was modulated by an 8 Mbit/s pseudo-random bit stream and had a noise bandwidth of 5.7 MHz; it was transmitted to the same transponder as the two IDR carriers, at a centre frequency mid-way between them. The interference peaks were generated one at a time, when required, and otherwise the interference level was at least 25 dB below maximum.

Two sizes of IDR carrier were included in the exercise, i.e. 64 kbit/s and 2 048 kbit/s information rate. The spectrum of the interference signal completely overlapped the spectra of the two IDR carriers in both cases. However, the width of the band between the edges of the noise bandwidths and the edges of the allocated bandwidths of the IDR carriers was 24.8 kHz in the case of the 64 kbit/s carriers, and 637.2 kHz in the case of the 2 048 kbit/s carriers. There was therefore adequate bandwidth for measurement of the power density of the received interference signal within the inter-carrier guardband, provided that the system noise density was also measured in the guardband to ensure that the contributions of the tails of the IDR carrier spectra were included. Examples of the spectra of the IDR carriers are shown in Fig. 4, and of the interference signal in Fig. 5.

Calculations were carried out to ensure that, for the transponder back-off concerned, non-linearity would have negligible impact on the accuracy of the measurements.

In order to confirm the feasibility of measuring epfd$_{\downarrow}$ peaks in the case of a very large antenna, some of the trials were repeated using the 19 m antenna to receive the carriers and the interference signal.

The main measurements were conducted with the two IDR carriers having the nominal INTELSAT parameters for transmission and reception by the sizes of earth station antenna involved. However, since this led to clear-air C/N ratios at the input to the demodulator of the order of 14-17 dB, a few of the measurements were repeated with the IDR carrier e.i.r.p.'s reduced to correspond to C/N ratios around 10 dB, in order to represent links to earth stations in dry areas operating with small rain margins and hence closer to the sync-loss threshold.

FIGURE 4

Spectrum analyser trace of 2 × 64 kbit/s carrier spectra

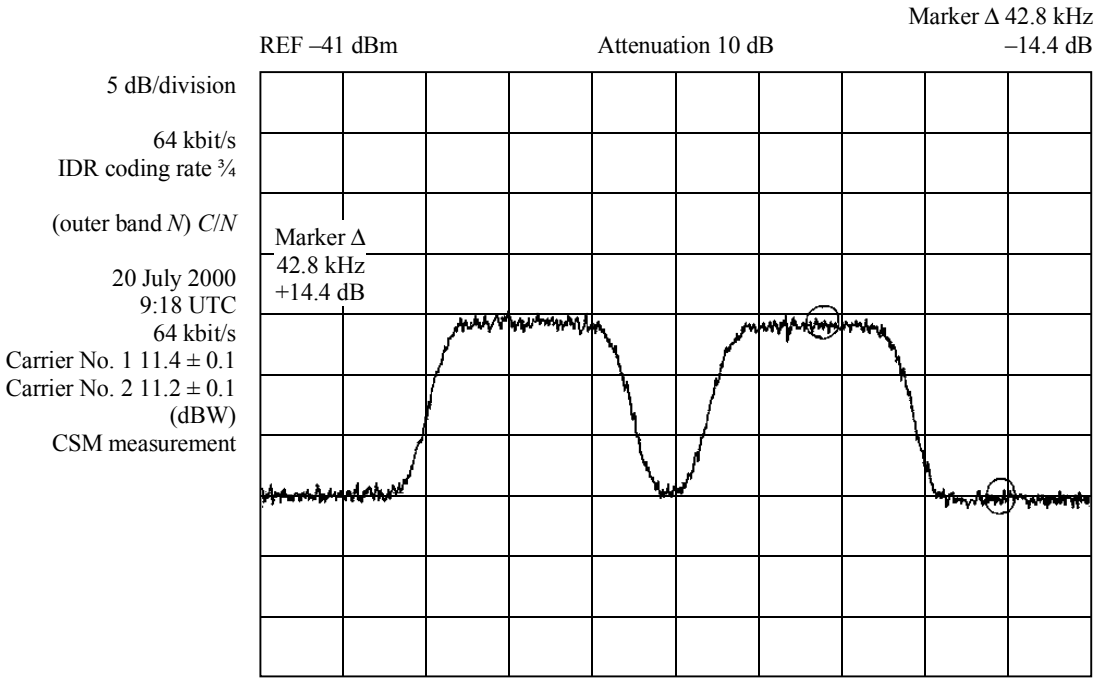

RBW: resolution bandwidth
REF: reference power level
VBW: video bandwidth

1558-04

FIGURE 5

Spectrum analyser trace of broadband interference signal

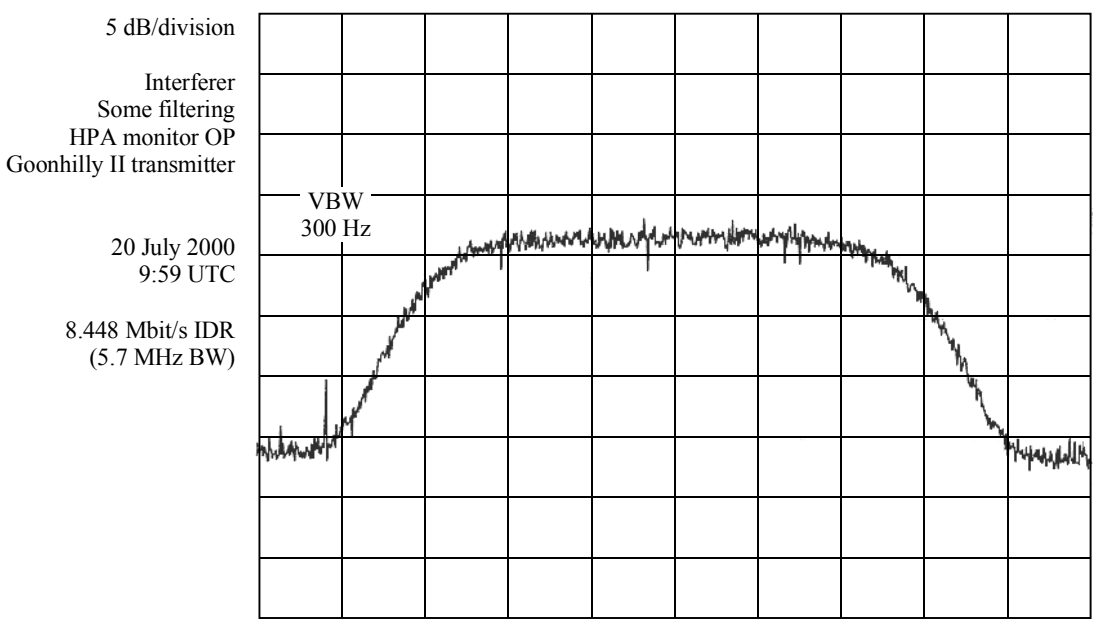

GHY: Goonhilly earth station
HPA: high power amplifier
OP: output power

1558-05

Each of the main measurements was carried out for several different interference peak levels. The first was a level near to the operational epfd↓ limit, followed by 3 dB above that level and then 6 dB above it. Then by trial and error, the level in some cases, at which an interference peak would cause loss of synchronization in the demodulator was determined, and in a few cases the level was determined below which masking by the system noise made reasonably accurate measurement impracticable.

For each series of measurements the IF receive level of the 5.5 m terminal (and of the 19 m terminal when appropriate) was re-calibrated via the CSM terminal, thus ensuring the best practicable accuracy.

Two variants of Method 2 were tested, each of the main measurements being first carried out using Method 2A, and subsequently repeated using Method 2B.

Method 2A: Prior to each series of measurements the IF received level of one of the IDR carriers was calibrated via the CSM station. The carrier was measured at the well-calibrated CSM station and hence the satellite e.i.r.p. toward that station was determined. Knowing that the satellite antenna gain toward Goonhilly is 5.5 dB lower than the gain toward the CSM station, and knowing the path length from the satellite to Goonhilly, the CSM station controller was able to state the pfd of the carrier at the Goonhilly antenna concerned. The corresponding IF receive level at Goonhilly was noted, and used as a reference level for the measurement, at Goonhilly, of the levels of the two carriers, C, the level of the system noise, N, and the level of the system noise plus the maximum interference, I, when a peak was received ($N + I$). These measurements were made manually, by viewing the display of a suitably adjusted spectrum analyser, and the epfd↓ level was calculated from the results.

Method 2B: Prior to each series of measurements an unmodulated pilot carrier was transmitted by a 3.7 m terminal in the guardband between the two IDR carriers, and received by both the 5.5 m terminal and the CSM station. This enabled the Goonhilly IF receive levels to be calibrated in the same way as in Method 2A, but using the received level of the pilot as the reference level. N and $N + I$ were measured with an automated set-up. Automation of the method was accomplished using equipment readily available at earth stations, and the spectrum analyser was controlled with software using HP VEE. The automated process uses the rise and fall slopes of the interference peak (video) output from the spectrum analyser to trigger the capture of the trace by a computer, which then calculated the peak epfd↓ from the N and $N + I$ levels. This was an important feature as an automated set-up will be essential for rarely occurring interfering peaks. An example print-out is shown in Fig. 6.

The recorded interference pulse in this example is about six seconds in duration and this matches the amplitude/time profile of the interference from a non-GSO satellite at 1 470 km altitude and 53° inclination during a pass through the beam centre of a 5.5 m earth station antenna located at Goonhilly and operating to a GSO satellite at 342° E. Note that once the peak of the pulse and the level of the noise floor have been clearly identified and captured, data points beyond that pulse do not need to be retained – this can be clearly seen in the graphical record of the interference pulse.

Since both Method 2A and Method 2B obtain the maximum interference level, I, and hence the peak epfd↓, from a measurement of N immediately followed by a measurement of $N + I$, and both quantities follow the same path from beyond the atmosphere to the IF measurement point, the measurement accuracy is equal to the accuracy of the latest calibration. The only unknown is the precise atmospheric attenuation at the time of the measurement, and as a check on this one of the satellite's telemetry beacons in the 11 GHz band was measured at Goonhilly and at the CSM station several times each day. In fact there were clear skies over both Goonhilly and Fucino throughout the week of measurements, and the beacon measurements indicated very little variation in the atmospheric loss.

FIGURE 6

Example of the computer print-out from the automated measurement of non-GSO epfd$_{\downarrow}$ using Method 2B

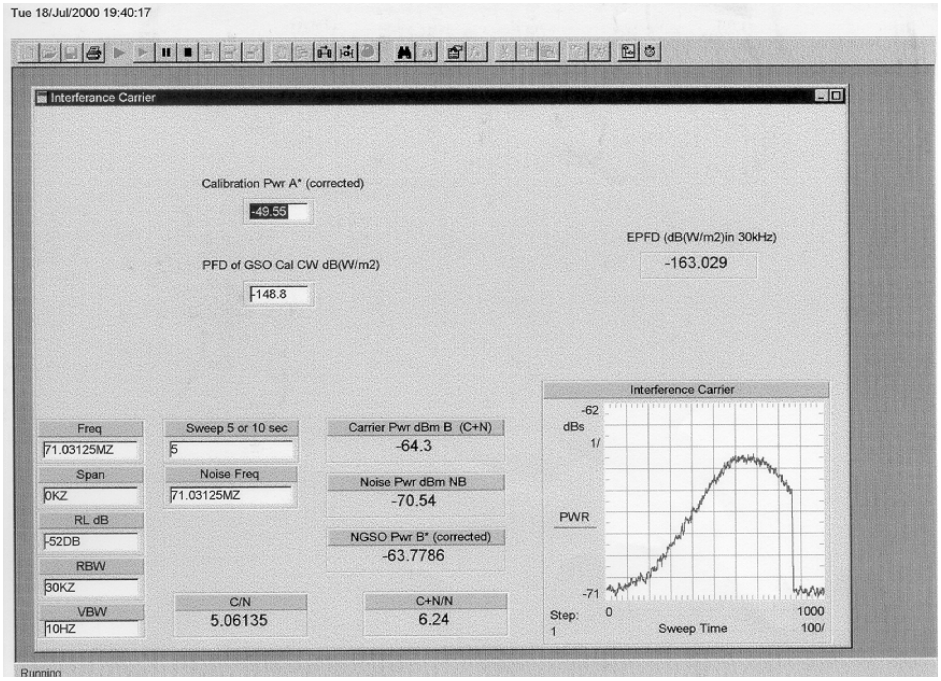

1558-06

3.6.2 Results and discussion

The results for the various permutations of antenna size, carrier parameters and measurement method are presented in summary form in Table 2.

The exercise provided practical confirmation that it is possible to measure short duration, infrequently occurring peaks of interference from a non-GSO constellation to an earth station in a GSO network, if the levels of those peaks are of similar order to the operational limit. Furthermore, this was done without interruption to the affected carrier, using a spectrum analyser such as may be found in many operational earth stations.

In Table 2, the fifth column indicates the number of measurements of epfd$_{\downarrow}$ carried out at Goonhilly for each set of circumstances, and the average of those measurements is contained in the sixth column. The spread of results relative to that average is shown in the penultimate column. The following observations are made:

– In those cases where a direct comparison can be made between the same measurement using Methods 2A and 2B, the differences in the average epfd$_{\downarrow}$ are small (between 0.07 dB and 0.38 dB). Differences of up to 0.6 dB were found in individual trials, thought to be due to the tendency for the manual method to take the average of a noisy spectrum analyser trace, and the automated method to respond to local peaks in the trace. It is considered that the results of the two methods are sufficiently close for each to corroborate the other.

TABLE 2

Summary results table

Receive antenna diameter	GSO carrier combinaison	Carrier *C/N* (dB)	Method	Number of trials	Average epfd↓ measured (dB(W/(m^2 · 40 kHz)))	Spread value (dB)	Spectrum analyser settings
5.5 m	2 × 2 Mbit/s	17	2A	7	−164.92	±0.59	VBW = 10 Hz Span = 0 RBW = 30 kHz
			2B	11	−164.85	±0.26	
			2A	6	−158.68	±0.2	
			2B	3	−158.80	±0.16	
			2A	6	−161.47	±0.28	
		10.3	2A	5	−164.82	±0.35	
				6	−161.54	±0.18	
				6	−158.52	±0.07	
		12	2B	1	−162.44	–	
				1	−165.77	–	
				1	−166.4	–	
				1	−166.82	–	
	2 × 64 kbit/s	17	2A	5	−165.11	±0.4	VBW = 1 Hz Span = 0 RBW = 3 kHz
			2B	8	−164.99	±0.39	
			2A	6	−162.11	±0.42	
			2B	5	−161.81	±0.15	
			2A	6	−159.13	±0.24	
			2B	4	−158.93	±0.09	
			2A	4	−161.59(1)	±0.11	
			2B	4	−161.21(1)	±0.19	
19 m	2 × 2 Mbit/s	10.3	2A	5	−168.62	±0.2	VBW = 10 Hz Span = 0 RBW = 30 kHz
				5	−165.67	±0.23	
				5	−162.55	±0.09	
		12	2B	5	−168.46	±0.2	
				5	−165.88	±0.15	
				5	−162.80	±0.1	
	2 × 64 kbit/s	14	2B	3	−167.64	±0.33	VBW = 10 Hz Span = 0 RBW = 30 kHz

(1) epfd↓ level at which the loss of synchronization occurs.

– The spread in the Goonhilly epfd↓ measurements in the multiple trials ranges from ±0.07 dB to ±0.59 dB (average 0.22 dB) over all permutations. Thus the short-term repeatability of the methods can be said to be good. Furthermore, a Method 2B measurement for the 2 × 2 Mbit/s carriers at C/N = 17 dB was repeated four days later for the same interference e.i.r.p. value measured by the CSM station, and the Goonhilly epfd↓ results differed only from −165.08 dB(W/(m^2 · 40 kHz)) ± 0.22 to −164.84 dB(W/(m^2 · 40 kHz)) ± 0.25. Hence the medium-term repeatability was also good.

– One factor which might impact on the long-term repeatability of results is the impact on CSM calibration of any changes in the satellite spot beam gain profile. For an INTELSAT satellite the gain contours are accurately and exhaustively measured soon after launch, and periodic spot checks are made in various locations during the operational life of the satellite. Nevertheless the difference between the gain towards the CSM and the gain towards the measurement point might be subject to long-term change, and an appropriate allowance should be made in the error budget for epfd↓ measurements.

The following further points of significance emerged during the course of the exercise:

– The present measurements were carried out via the antenna receiving the affected carrier – an operational antenna. An alternative possibility would be to use a separate, transportable antenna, well calibrated and pointed toward the GSO satellite concerned. For economic and practical reasons this would be a relatively small antenna, and thus in most cases its beamwidth would be wider than that of the antenna receiving the non-GSO interference. Hence its beam would be intercepted by a non-GSO satellite at times when the operational antenna's beam would not be intercepted. This and other difficulties linked to the use of such a separate antenna are addressed in Recommendation ITU-R S.1554.

– To help to minimize measurement errors the cooperation of the CSM station controller and the CSM station at Fucino was arranged for this exercise. It is conceivable that such cooperation might be forthcoming in operational circumstances for any earth station operating to an INTELSAT satellite, and it is assumed that other GSO operators have some form of CSM station. Self-calibration would be an alternative, but the accuracy of the measurements might be less in that case.

– The advantage of an automated measurement set-up, such as that used in Method 2B, is that the need is avoided to have staff on stand-by once every week or so, watching for an isolated interference peak whose duration may be less than 1 s. Up-to-date ephemeris data for the non-GSO FSS systems would identify the times of in-line passes reasonably accurately, but the highest interference peaks may not occur during every in-line event. Even with an automated measurement set-up, if third-party (e.g. CSM station controller) assistance for calibration is required, it will be necessary for the third party to be available at a time reasonably close to the in-line event time. But there appears to be no reason why the calibration should not be done shortly after the event, rather than shortly before it, which in principle would allow the third party to be alerted by a trigger which would be automatically activated if the measured epfd↓ had exceeded the operational limit.

– This exercise showed that reliable and reasonably accurate measurements of epfd↓ may be made using a spectrum analyser of a type commonly used in earth stations either manually, or automatically with the aid of a PC. However, the settings of the analyser's resolution bandwidth, video bandwidth and sweep rate are critical to the measurements, especially in cases where the GSO carrier bit rates, and hence the measurement bandwidth, are low and/or the width of the interference peak is small. An alternative to the spectrum analyser is an approach based on a DSP described elsewhere in Section 3, where more samples during

the interference pulse could be taken and stored prior to analysis. The internal stability of such a device would potentially be better than that of a spectrum analyser, and human error in manual readings would be reduced. A disadvantage of the DSP approach might be the development and procurement costs involved.

– It is conceivable that earth stations in dry areas could be receiving several carriers operating with low *C*/*N* margins, and hence be at risk of loss of synchronization at more than one frequency within the FSS space-to-Earth allocation. But owing to variations in the traffic loading of the non-GSO system, loss of synchronization may occur for different carriers during different in-line events. Hence the operator of such an earth station might wish to make epfd↓ measurements at more than one frequency during a single in-line event. In principle this could be done, but the complexity would be greater and there may be difficulties in making several sequential measurements within the duration of a short interference pulse. The DSP approach may be preferable in these circumstances.

3.6.3 Measurement errors

During the exercise the following potential sources of error were identified. Assessments of each uncertainty in terms of its possible error contribution are given, and these can be statistically combined to produce the overall measurement accuracy to a good level of confidence. The error contributions are further discussed in Recommendation ITU-R S.1554.

a) Uncertainty in the CSM station receive measurement (±0.45 dB).

b) Uncertainty in the CSM station calibration of Goonhilly receive level (±0.56 dB).

c) Uncertainty in the difference in received level of a signal at the frequency of the affected carrier and at the centre frequency of an adjacent guardband (difference likely to be negligible).

d) Uncertainty in making the spectrum analyser measurement of $(I + N)/N$ (±0.75 dB).

3.7 Measurement precautions and uncertainties

It should be noted that in the case of spectrum analysers, resolution bandwidths are usually available in discrete steps. It would be preferable to measure power densities using the same 40 kHz bandwidth as that in which the epfd↓ levels are specified, however the closest resolution bandwidth available on most spectrum analysers is 30 kHz. Using the power and noise density measurement technique it may be necessary to choose a different reference bandwidth for measurement of epfd↓ levels than that in the tables of RR Article 22 and simply scale the measured level to the required level of compliance. With a digital signal processing measurement as described below, the carrier and noise power measurements can be directly calculated over a bandwidth of 40 kHz.

Attention must be paid to the measurement of the $(C + N)/N$ on the spectrum analyser in order to derive the *C*/*N*. It has been found that the reference bandwidth, video bandwidth, span and sweep time of the spectrum analyser can give different results for the measurement of the $(C + N)/N$ in the guardband between the two carriers. In all spectrum analyser measurements it should be verified that these settings are not changing the accuracy of the measurements, due to too much time or bandwidth averaging.

In addition the guardband between carriers are not always wide enough to allow measurement of the actual noise under the carrier. For example, in the measurements described in Section 3.6 the guardband between the 2×64 kbit/s carriers was 24.8 kHz (67.5 – 42.7 kHz) and 572.5 kHz (2 002.5 – 1 430 kHz) for the 2×2 Mbit/s carriers. For the 2×64 kbit/s carriers a 3 kHz bandwidth should be used and for the 2×2 Mbit/s carrier a reference bandwidth of 30 kHz should be used.

In a situation where the transponder is fully loaded the noise measurements would be taken adjacent to the interfered with carriers. However, if the guardband is too narrow the noise measurement could be 1-2 dB higher than the real thermal noise, N, under the carrier. If N' is the noise level in the guardband, the correction that would be required to any epfd↓ measurements is the difference in the noise level, N', when $(C + N)/N'$ is not equal to $(C + N)/N$.

The chart in Fig. 7 shows the correction factor that should be used depending on the difference between $(C + N)/N'$ and $(C + N)/N$.

FIGURE 7

Correction factor for $(C + N)/N$ measurements taking into account noise in the guardband between adjacent GSO carriers

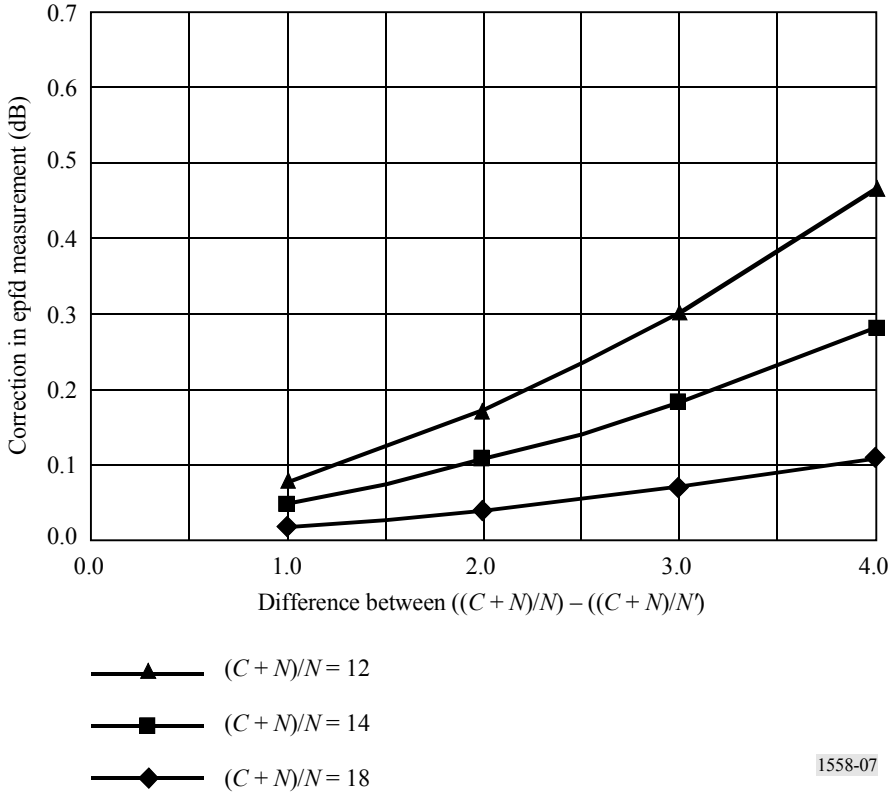

As can be seen in Fig. 7 the correction for a $(C + N)/N$ of 12 dB would be 0.2-0.3 dB if the $(C + N)/N'$ were 2-3 dB less respectively.

It is important to ensure that the spectrum analyser (SA) noise floor is as low as possible to prevent any restriction on the dynamic range of the measurements. Typically for accurate IF level measurements the spectrum analyser noise floor should be at least 20 dB below the noise floor of the receive signal. The linearity of the spectrum analyser over the measurement range should be checked at the specific settings used for the $(C + N)/N$ measurements. In other words the accuracy of the spectrum analyser over say 10 dB could be impaired if the amplifiers in the SA are at the end of their range. It is also important to ensure that the appropriate correction factors for the spectrum analyser are taken into account when measuring noise-like signals.

The required calibration and uncertainties for this measurement procedure are discussed further in Recommendation ITU-R S.1554.

3.8 Conclusions concerning the application of the methods described in Section 3

Verification of exceedences of an operational limit by measurement at an earth station in service, without interruption of traffic, is feasible, within certain tolerances. Such measurements may be carried out using conventional test equipment, and it is practicable for this to be done automatically.

If Method 1 followed by epfd↓ measurements by a method such as Method 2A or 2B described in Section 3 are carried out carefully the net root sum squared (RSS) error in the results is likely to be of the order of ±1.0 dB (see Recommendation ITU-R S.1554).

A non-GSO constellation creating peaks of interference to an earth station in a GSO network can be readily identified by using ephemeris data to predict the times of the in-line passes, and a suitable receiver to detect a telemetry carrier or other continuous signal transmitted by each non-GSO satellite in the constellation. However, if the exact time of the interference peak is logged (see extreme top of Fig. 6) the automated epfd↓ measurement itself could be used for this purpose, thus avoiding the need for a separate antenna or receiver.

Difficulties identified during the exercise described herein included:

– If a spectrum analyser is used as the measuring device in an automated test set-up, its settings may be critical for the shorter epfd↓ peaks, which occur for very large earth station antennas. In the case of manual measurements, taking readings from a spectrum analyser involves human error. A special purpose DSP-based device could be used instead, which potentially would obviate these difficulties but at greater cost. The DSP allows the storage of the data if further analysis is required.

– The accuracy of measuring epfd↓ peaks may be improved if the received level of the affected earth station can be calibrated by a CSM station located in the same satellite beam. However, earth stations in some networks may not have access to a CSM station. In such cases the earth station may either rely on self-calibration, or make use of a purpose-designed, well-calibrated, small-dish, transportable terminal, probably at less accuracy and/or greater cost.

– A systematic difference of the order of 0.6 dB was found between epfd↓ levels derived from CSM measurement of the downlink e.i.r.p. of the interfering signal, and measurements of the same signal via the Goonhilly receive system whose receive level had just been calibrated by the CSM station. It is believed that this difference will be eliminated with further work.

Although this exercise was carried out in the 11 GHz band, and with interference peaks typical of a low Earth orbit (LEO) constellation of 1 470 km altitude, there is no reason to doubt that the measurement methods described would be feasible in the case of 18 GHz or 20 GHz systems, and/or with interference peaks typical of medium Earth orbit (MEO) systems. For non-GSO constellations having altitudes of the order of 700 km in either band, however, the duration of each interference peak would be shorter, and this may create difficulties for measurements involving the larger earth station antennas.

4 Method 3: Correlation techniques

The measurement procedure proposed in this Section provides a measurement of the non-GSO signal power level into an operating GSO carrier in cases where the non-GSO signal is well below the operating GSO carrier (up to 20 dB in the example studied).

4.1 Principle of the method

This procedure can be applied to non-GSO systems using CDMA which may have a reference signal accessible under these conditions.

The following explanation is written for the case of a CDMA system. The exact adaptation of these techniques to time division multiple access (TDMA), FDMA and combinations of access modes needs further study.

The principle of the method is to correlate a portion of the signal coming into the operational GSO earth station at the time of a loss of synchronization with a known signal. This technique has the advantage of being able to detect the non-GSO interference even in the presence of the GSO signal and noise. The ability of this technique to detect the very low interference levels is due to the processing gain achieved through the correlation. The amount of processing gain is a function of the integration time and correlation technique used.

It has to be noted that this method has assumed that the GSO earth station is interfered with by a side lobe of a single beam of an non-GSO satellite. Further studies are required to determine the feasibility of such methods in the case of side lobes of several beams causing interference into the GSO earth station.

4.1.1 Cyclic auto-correlation techniques

The measurement of the power level of the non-GSO carrier level in this technique is achieved through the auto-correlation of the recorded signal in a cyclic manner.

The cyclic auto-correlation calculation of a signal $s(t)$ is based on a fast Fourier transform (FFT) transformation of the signal auto-correlation $\Gamma_s(t, \tau)$ of the signal $s(t)$ in the plan defined by one time variable and one frequency variable. The chip rate R_c of the non-GSO signal is used as a discriminant signal to correlate the non-GSO signal with itself and achieve a sufficient increase in gain.

The efficiency and accuracy of this method depends on the integration time that can be obtained for the non-GSO signal.

The advantage of this method is that it provides a direct measurement of the non-GSO carrier level interfering into the operating GSO carrier. It is therefore fully representative of the traffic in a single beam of the non-GSO carrier satellite at the time of the loss of synchronization.

A study of one specific interference scenario demonstrated that the interference can be measured for $C_{GSO}/I_{non\text{-}GSO}$ up to 10 dB.

The accuracy associated with this technique requires further studies.

4.1.2 Auto-correlation techniques

Auto-correlation techniques correlate the recorded signal with a delayed version of itself. This method does not directly provide the measurement of the non-GSO carrier power level but the measurement of a reference signal.

The estimation of the non-GSO carrier level has to be estimated using a relation providing the power level ratio between the non-GSO reference signal and the non-GSO carrier signal. The relationship of the reference level to non-GSO carrier level accuracy of this estimation is discussed in § 4.1.4.

The efficiency of the auto-correlation technique in terms of $C_{GSO}/I_{non\text{-}GSO}$ and its associated accuracy require further studies.

4.1.3 Cross-correlation techniques

Cross-correlation techniques correlate the recorded signal with a reference signal that does not need to be specific. As for the auto-correlation techniques, cross-correlation techniques do not directly provide the measurement of the non-GSO carrier power level but the measurement of a reference signal. The estimation of the non-GSO carrier level has to be estimated using a relation providing the power level ratio between the non-GSO reference signal and the non-GSO carrier signal. The relationship of the reference level to non-GSO carrier level is discussed in § 4.1.4.

Using simulations on a representative CDMA non-GSO system interfering into an operational GSO earth station with a $C_{GSO}/I_{non\text{-}GSO}$ of 20 dB and a required 60 dB gain on the reference signal, it has been shown that an accuracy of at best 1 dB can be achieved on the measurement of the non-GSO reference signal (without taking into account the accuracy of calibration of the GSO reception chain).

4.1.4 Relation of the power level between the non-GSO reference signal and the non-GSO carrier signal

The relation of the power level between the non-GSO reference signal and the non-GSO carrier signal can be achieved in two ways:

a) by observing the average ratio between the non-GSO reference signal and the carrier levels using a separate test antenna pointing at the non-GSO space station main beam. The problem with this approach is that it provides information on the ratio between the non-GSO reference signal level and the non-GSO carrier level that is representative of the traffic of a particular non-GSO satellite at a given time, in a given beam but which may not be representative of the traffic served by the non-GSO satellite causing interference in the beam of the GSO earth station, at the time of the synchronization loss; or

b) by providing the maximum ratio between the non-GSO reference signal and the carrier levels by the non-GSO operator. The problem of this approach is that it may overestimate the non-GSO carrier signal. In addition it may be difficult for the non-GSO system to provide a fixed value of the pfd level of the non-GSO reference signal with respect to the traffic loading as there may be uncertainty regarding the influence of the traffic level on the reference signal level.

Further studies would be required to determine the accuracy of each approach, but b) appears to be preferable.

4.2 Test set-up description

The test set-up associated with this method is common to the different correlation approaches which are proposed.

The location of the measurement system should be on the premises of the GSO earth station so that the antenna and the LNA are common to the GSO earth station receiving chain and the measurement system.

FIGURE 8

Location of the measurement system in the GSO reception chain

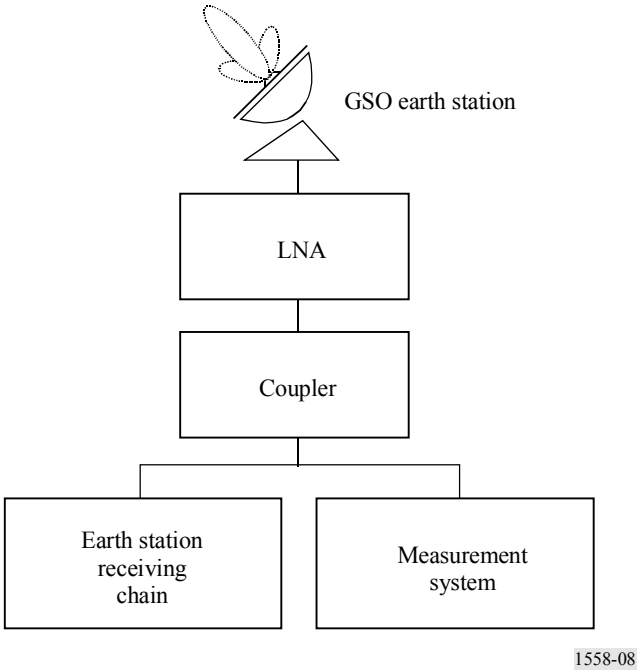

The block diagram of the test set-up associated with this method is provided in Fig. 9:

FIGURE 9

Non-GSO power level measurement test setup

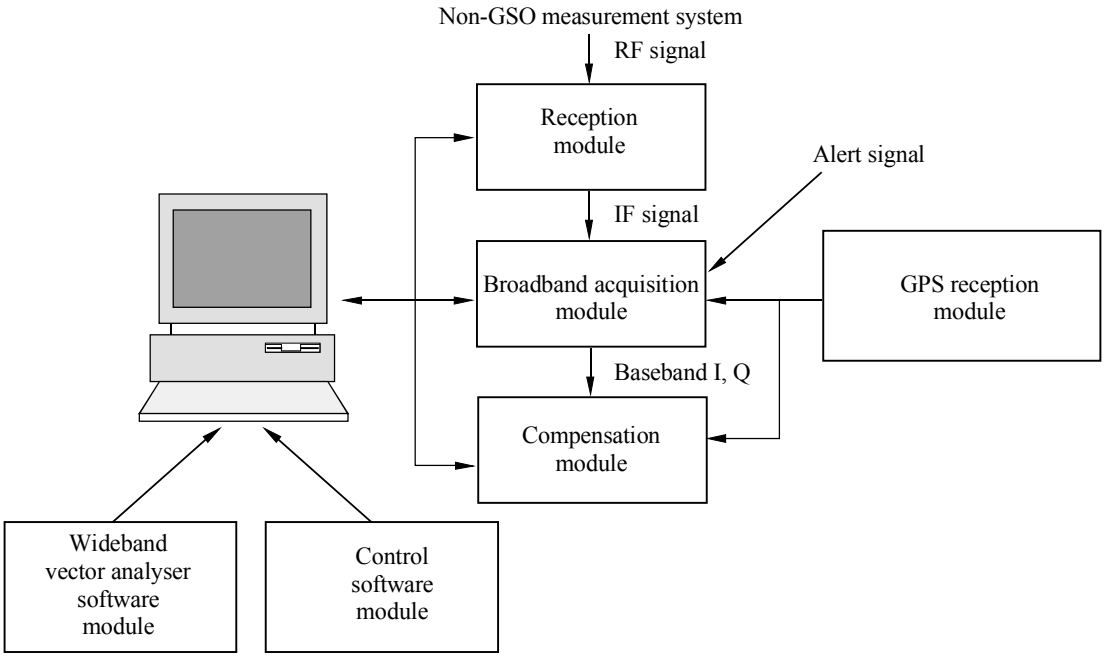

GPS: global positioning system

The measurement system comprises:

– A reception module which translates the necessary bandwidth portion of the incoming RF signal into a standard IF signal.

– A broadband acquisition module, which digitizes, translates into baseband the IF signal, and then samples and stores the baseband signal.

– A GPS reception module, which delivers the precise time of recording of the non-GSO signal.

– A compensation module which performs the Doppler frequency and timing compensation on the broadband signal.

– A computing unit for the operation of the measurement system which is based on two software modules:

  – a wideband software vector analyser which allows the detection and measurement of non-GSO interfering signal with a GSO signal;

  – a control software which allows the remote control of the chain by data link (RS232, IEEE488, Ethernet).

4.3 Calculation of the non-GSO epfd↓ level

The measurement procedure proposed in § 4.1 provides the non-GSO power level at the output of the coupler in the GSO reception chain (see Fig. 8). In order for the GSO operator to verify the compliance of the non-GSO carrier power level with the operational limits provided in RR Tables 22-4A and 22-4B, it is necessary to translate the non-GSO power level into the epfd↓ level that is actually received at the GSO earth station.

The following provides the calculations necessary to express the non-GSO power level measured in § 4.1, into the non-GSO epfd↓ level received at the input of the operational GSO earth station.

The received non-GSO power at the antenna aperture, p_{input} (W), is provided by the following equation:

$$p_{input} = \left[\frac{p_e}{4\pi d^2}\right] \cdot \left[g_{ant}\,\frac{\lambda^2}{4\pi}\right] = \Phi \cdot s_{eff} \qquad \text{W}$$

where:

p_e: emitted power (W)

λ: wavelength (m)

d: satellite to earth station distance (m)

Φ: pfd at the antenna input (W)

g_{ant}: antenna receive gain (dBi)

s_{eff}: equivalent antenna aperture area (m^2).

The received non-GSO power at the coupler output is provided by the following equation:

$$P_{output} = P_{input} + G_{LNA} - L \qquad \text{dBW}$$

where:

G_{LNA}: low noise amplifier gain (dB)

L: losses between the LNA output and the measurement system monitoring point (dB).

The correlation technique described in § 4.1 gives the power level of the non-GSO signal in 40 kHz. Knowing the output received signal after antenna, and the LNA amplifier gain and losses in the measurement system, the epfd↓ generated by the non-GSO system into the GSO earth station is given by the following expression (NOTE 1 – When interference epfd↓ (Φ) is received on-axis, it is effectively a pfd (Φ)):

$$10 \log_{10} \Phi = 10 \log_{10} P_{non\text{-}GSO\text{-}40\ kHz} - 10 \log_{10} (s_{eff}) - G_{LNA} + L + 10 \log_{10} (B/40) \quad \text{dB(W/(m}^2 \cdot \text{40 kHz))}$$

where B is the non-GSO carrier bandwidth (kHz).

In the above equation, the term $-10 \log_{10} (s_{eff}) - G_{LNA} + L$ has to be determined by the calibration process described in the following section.

4.4 Receive earth station calibration

4.4.1 Introduction

The purpose of calibrating the receive earth station is to provide a conversion factor that enables the translation of power measurements taken at an RF or IF point in the receive chain into an epfd value at the receive antenna aperture. For example, the peak power level of a signal associated with a non-GSO interferer is measured at the output of the earth terminal down-converter, as shown in Fig. 10. The power level measurement is made either in absolute terms, or relative to some known reference level. In either case, the gain along the signal path between the receive antenna aperture and the down-converter output, as a function of frequency, must be subtracted from the measured value to arrive at a flux-density. Several methods that could be used to calibrate the antenna and receive chain are summarized below.

FIGURE 10

Injected carrier receive earth terminal calibration

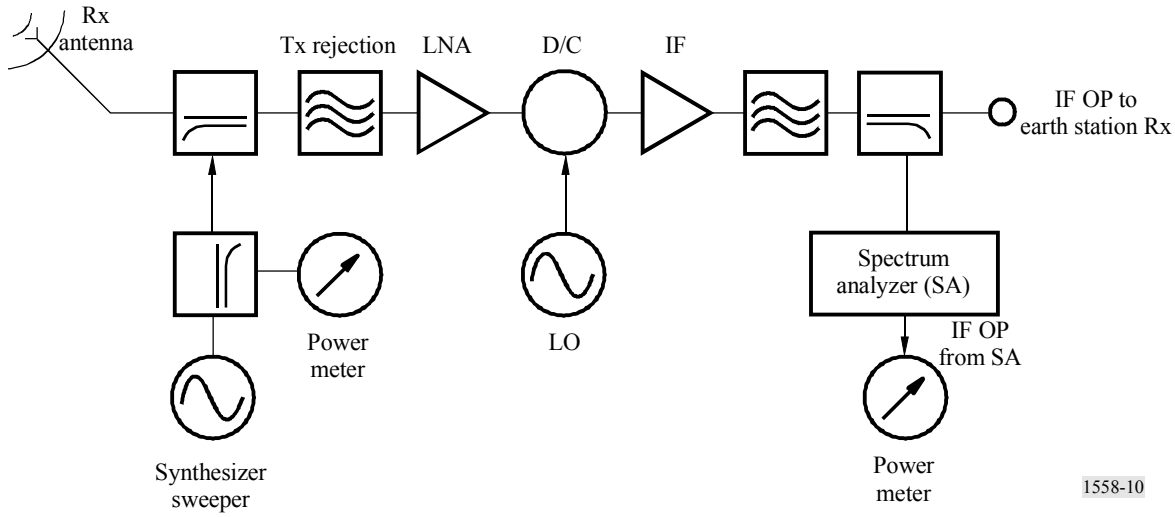

4.4.2 Calibration methods

4.4.2.1 Injected carrier calibration method

With the objective of providing the greatest accuracy possible for measuring the epfd↓, a fully calibrated receive earth terminal is required. The term, fully calibrated, constitutes that both the receive antenna gain at the waveguide output flange as well as the conversion gain of the LNA or

block-down converter, low noise block (LNB) chain, are known over the operation bandwidth of the earth station. The conversion factor is determined by the summation of all of the gain transfer characteristics.

If such calibration data is unavailable for the LNB chain, then a test setup such as that shown in Fig. 10 is required in order to calibrate the LNB chain. This block diagram assumes that a means is available for injecting a continuous wave (CW) carrier into the signal path of the receive chain and observing the injected carrier level at the output. Because a coupler is required between the antenna and LNA, it is likely that this scheme would only be used for a dedicated, standalone earth station, an in-orbit test terminal, or an earth station that is offline for reconfiguration.

By injecting a swept frequency CW carrier prior to the LNB chain, the path through the LNB chain can be completely characterized in terms of frequency-amplitude pairs. If the earth terminal is operating during the calibration, then a list of discrete frequencies must be selected for the calibration so as not to interfere with earth station operations. These results may then be stored in a calibration table to be used for subsequent data processing. In calibrating the LNB chain, linear operation of the LNA must be verified prior to the calibration measurement. The insertion loss and coupling factors of the directional couplers of Fig. 10 must be characterized prior to the calibration.

The single largest source of uncertainty in the measurement methods discussed here is associated with the receive earth terminal antenna. Several different methods exist for measuring the gain and G/T_S of an antenna, and with each comes an associated level of uncertainty.

The earth terminal antenna can be gain calibrated using one of several different means depending on the available time and resources, and the accuracy that is desired. At 14/11 GHz band frequencies, the radiostar method is employed for aperture diameters of at least 11 m. For antennas less than 11 m in diameter, the gain can be calculated using the pattern integration method or beamwidth approximation method. For much smaller antennas, the gain can be determined more accurately using the standard gain horn method.

4.4.2.2 Standard gain horn method

The standard gain horn (SGH) method is typically used for small apertures, and simply compares the antenna under test (AUT) with another antenna with known gain. This method is one of the most accurate amongst those discussed here, and has a total RSS error of approximately ±0.44 dB. However, this method is usually not practical for large apertures such as earth station antennas because of the large difference in gain between the AUT and SGH.

4.4.2.3 Pattern integration method

Antenna directivity can be determined by integrating and averaging several wide-angle radiation pattern cuts at a given frequency. Expected losses for factors such as root mean square surface tolerance, polarization purity, ohmic losses, pattern truncation, and spillover are subtracted from the directivity value to arrive at antenna gain at the waveguide output flange. Radiation pattern data must be obtained at several different frequencies to compute antenna gain over the band.

4.4.2.4 Beamwidth approximation method

The beamwidth approximation method is typically used for reflector antennas that are known to have an efficiency in the range of 65% to 70%. The methodology requires the measurement of the beamwidth of the antenna radiation pattern, and applies a formula to calculate the gain, and it always includes an approximation error term of 0.40 dB. The total RSS error is approximately ±0.55 dB. It also requires a separate feed loss measurement.

4.4.2.5 Radiostar method

Due to recent advances in the calibration of flux densities emitted by radiostars, the most accurate antenna gain calibration technique for antennas is the radiostar method, provided the antenna has a sufficiently large aperture and the test frequency is sufficiently high. The radiostar method is actually composed of a pair of measurements: one to measure gain, and the other to measure system noise temperature, T_S, at a given elevation angle. The total RSS uncertainty associated with the gain measurement is ±0.23 dB.

4.4.2.6 Calibrated reference earth station method

The above calibration procedures require out-of-service testing of the earth station which is not always feasible when the earth station is carrying a large amount of essential traffic. Another means of calibrating the receive earth station is to measure the power/pfd of a test carrier at a calibrated reference earth station, and knowing the off-set gain of the satellite transmit antenna to both the calibrated reference antenna and the test receive earth station, the gain of the antenna and receive chain can be calculated.

INTELSAT utilizes several calibrated earth stations for CSM, or in-orbit testing (IOT). These earth stations provide very accurate measurements of the downlink carrier or test signals from the satellite. In the case of the CSM earth stations the level of each of the traffic carriers on a transponder is carefully monitored to ensure the transponders are operating with the proper input and output back-offs. In the case of the IOT earth stations, the receive levels from the satellite are accurately measured for the in-orbit test verification of the satellite during acceptance tests.

4.4.3 Receive earth terminal calibration uncertainty

Any measurement has a level of uncertainty associated with it. The accuracy of the measurement methods discussed here depend upon:

– Frequency of operation. Measurement errors can be expected to increase with frequency.

– Availability of accurately calibrated radio source (i.e. radiostar) at the test site, and a sufficiently large antenna to use the radiostar method. For example, at 11 GHz band, an aperture size of at least 11 m is required to perform a gain and G/T_S measurement using the radiostar method.

– Calibration of inserted feed networks, couplers, and/or transmission lines.

– Antenna pointing and alignment.

– Mismatches in the test setup, including voltage standing wave ratio (VSWR) changes caused by the test equipment.

– Clear, calm weather.

Table 3 lists typical uncertainties associated with the various antenna gain measurement techniques, the uncertainty associated with the power meter instrument that would be required in the receive chain calibration procedure described above and the uncertainty associated with performing the *C*/*N* measurement described above.

TABLE 3

Component measurement uncertainties

Antenna gain	(dB)
Radiostar method	±0.23
SGH	±0.44
Pattern integration method	±0.55
Beamwidth approximation method	±0.55
Power meters	
Power meter uncertainties	±0.20
DSS uncertainty	±0.25

Table 4 summarizes typical values for the total worst case and RSS uncertainties for the injected carrier calibration procedure, which requires one of the antenna gain calibration components, and two times the power meter uncertainty components (since two power meters are used to make a relative, not absolute, power measurement).

TABLE 4

Total measurement uncertainties

	Total worst-case uncertainty (dB)	**Total RSS uncertainty (dB)**
Radiostar	±0.88	±0.43
SGH	±1.09	±0.57
Pattern integration	±1.20	±0.65
Beamwidth approximation	±1.20	±0.65

An alternative method is to utilize the earth station G/T value which would be available from the standard earth station verification testing. Using the $(C + N)/N$ or $(I + N)/N$ measured values to derive the C/N or I/N, and the conversion equation given below, the pfd at the input to the antenna can be determined.

$$pfd = 10 \log\left(kb \frac{c}{n} \left(\frac{4\pi}{\lambda^2} \right) \frac{t_s}{g_r} \right) \qquad \text{dB(W/(m}^2 \cdot \text{40 kHz))}$$

where:

k: Boltzmann's constant (1.38×10^{-23} W/Hz/K)

b: reference bandwidth (40 kHz)

$\frac{c}{n}$: C/N, expressed as numerical ratio

λ: wavelength (m)

t_s: noise temperature of receiving earth stations (K)

g_r: on-axis receive gain of the earth station antenna (dBi).

It is assumed that T_s can be calculated or is equal to the receive earth station T. If the earth station G/T was derived using a radiostar method, the pfd measurement would have an RSS uncertainty of typically ±0.41 dB.

In the case of the calibrated reference earth station method, the typical pfd measurement at a CSM or IOT earth station has an uncertainty of approximately ±0.43 dB. Taking into account the uncertainties of the spacecraft antenna pattern, pointing errors and DSP measurements, the total RSS uncertainty would be approximately ±0.56 dB (e.g. § 3.6.3 b)).

The above measurement uncertainties cannot be avoided since the accuracy of actual RF or IF measurements at an operational earth station are constrained by the calibration tools available to the operator. To resolve such measurement uncertainties can be a time consuming and relatively expensive process for operational GSO FSS systems. The development of regulatory procedures relying on such operational measurements should take the margin for error into account.